ADVANCES IN ATMOSPHERIC SCIENCES, VOL. 22, NO. 2, 2005, 199–211

Interannual Meridional Displacement of the East Asian Upper-tropospheric Jet Stream in Summer

LIN Zhongda*[1,2] (林中达) and LU Riyu[1] (陆日宇)

[1] *Institute of Atmospheric Physics, Chinese Academy of Sciences, Beijing* 100080

[2] *Graduate School of the Chinese Academy of Sciences, Beijing* 100039

(Received 16 June 2004; revised 17 November 2004)

ABSTRACT

On the interannual timescale, the meridional displacement of the East Asian upper-tropospheric jet stream (EAJS) is significantly associated with the rainfall anomalies in East Asia in summer. In this study, using the data from the National Centers for Environmental Prediction-Department of Energy (NCEP/DOE) reanalysis-2 from 1979 to 2002, the authors investigate the interannual variations of the EAJS's meridional displacement in summer and their associations with the variations of the South Asian high (SAH) and the western North Pacific subtropical high (WNPSH), which are dominant circulation features in the upper and lower troposhere, respectively. The result from an EOF analysis shows that the meridional displacement is the most remarkable feature of the interannual variations of the EAJS in each month of summer and in summer as a whole. A composite analysis indicates that the summer (June-July-August, JJA) EAJS index, which is intended to depict the interannual meridional displacement of the EAJS, is not appropriate because the anomalies of the zonal wind at 200 hPa (U200) in July and August only, rather than in June, significantly contribute to the summer EAJS index. Thus, the index for each month in summer is defined according to the location of the EAJS core in each month. Composite analyses based on the monthly indexes show that corresponding to the monthly equatorward displacement of the EAJS, the South Asian high (SAH) extends southeastward clearly in July and August, and the western North Pacific subtropical high (WNPSH) withdraws southward in June and August.

Key words: East Asian jet stream, western North Pacific subtropical high, South Asian high, interannual variations, meridional displacement

1. Introduction

The East Asian jet stream (EAJS), which often refers to the upper-troposphere westerly jet stream over subtropical East Asia and the Western Pacific, is an extremely important synoptic and climatological factor over East Asia. During the past decades from the 1950s, much effort has been applied to studying the relationship between the EAJS and weather in Asia and the Pacific. It has been found that the EAJS is closely related to many synoptic phenomena, such as cyclongenesis, frontgenesis, blocking, and storm track activity (e.g., Palmen and Newton, 1969; Zeng, 1979; Kung and Chan, 1981; Dole and Black, 1990; Gao and Tao, 1991; Bell et al., 2000), which have been widely used for weather analysis and prediction in many Asian countries.

On seasonal timescales, it has been known that the shift of the EAJS is closely related to the abrupt seasonal transition of the monsoon over East Asia (Yeh et al., 1959). Neyama (1963) used wind observations in the upper troposphere at Marcus Island (24°17′N, 153°88′E) and found a close relationship between the date of the wind direction transition and the mei-yu rain season in Japan. Taking the year 1979 as an example, Tao and Chen (1987) demonstrated the association of the western North Pacific subtropical high (WNPSH) and the South Asian high (SAH) with the westerly jet in the upper troposphere during the onset of monsoon. Many other climate signals, such as SST anomalies in the tropical Pacific, accompanied with the change in EAJS are also suggested (Ding, 1992; Lau et al., 2000).

But on the interannual timescale, previous works have mainly focused on the association of the variations of the westerly jet stream in boreal winter

*E-mail: zdlin@mails.gscas.ac.cn

with the tropical heating (Lau and Boyle, 1987; Yang and Webster, 1990), Hadley circulation (Hou, 1998), and Asian-Pacific-American winter climate anomalies (Yang et al., 2002). Until recently, only several papers have mentioned the change of intensity and displacement of the EAJS in boreal summer. It was found that on the interannual scale, the variability of the westerly intensity is closely associated with the intensity of convective activity over the tropical region, which is located to the south of the westerly jet stream (Dong et al., 1999). Based on the correlation patterns of June-July-August (JJA) rainfall in Southeast Asia with 200-hPa zonal wind, Lau et al. (2000) found that the most prominent feature correlated with rainfall in Southeast Asia is the meridional displacement of the EAJS around 40°N oriented from 110°E to 150°E. Analyzing the associations with the interannual variations of the onset of the Changma, Lu et al. (2001) found that the EAJS is stronger and located relatively southward with respect to the later Changma onset. Moreover, Lu (2004) revealed that the variations in the EAJS's intensity and meridional displacement correspond to convection anomalies along the East Asian summer rainy belt, and the meridional displacement of the EAJS has a more intimate relationship with the East Asian summer rainfall than the intensity of the EAJS.

SAH is a semi-dominant feature of circulation in the upper troposphere and lower stratosphere, located around the latitude of 30°N over South Asia in boreal summer. The significant warming over the Tibetan Plateau resulting from latent heating and surface sensible heating in the late spring-early summer leads to the local anticyclonic disturbance in the upper troposphere (Zhang and Wu, 1999). Furthermore, Wu et al. (2002) found that the negative potential vorticity generated by heating in the upper layers over the Tibetan Plateau is balanced by the divergence of negative potential vorticity, which maintains a strong and stable SAH. On the interannual timescale, the zonal displacement of the SAH is strongly related to the climate anomalies in East Asia (Zhang et al., 2002). The relationship between the interannual variations of the SAH and the EAJS remains unclear.

It is still not well investigated how the EAJS is displaced in the meridional direction on the interannual timescale in boreal summer, although the impacts of the EAJS on the weather and winter climate over East Asia are greatly known. In the present study, we will examine the EAJS's meridional displacement, which will be shown to be the most remarkable feature of the EAJS's variations in boreal summer. The climatological features of the zonal wind at 200 hPa (U200) are presented in section 2. The circulation anomalies associated with the interannual meridional displacement of the EAJS in summer are examined in section 3. Finally, a summary is given in section 4.

2. U200 Climatology

The data used in this study are the winds, geopotential height with a spatial resolution of 2.5° × 2.5° from the reanalysis-2 product of the National Centers for Environmental Prediction/Department of Energy (NCEP/DOE) Atmospheric Model Intercomparison Project (AMIP-II) for 1979–2002 (Kanamitsu et al., 2002), which is based on the widely used NCEP/NCAR Reanalysis. The monthly mean data are used in this study.

Figure 1 shows the climatological zonal wind at 200 hPa (U200) for June, July, August and the JJA mean, respectively. The upper-tropospheric jet stream is basically zonally oriented over East Asia, and has southwest-northeast tilt over the North Pacific. However, there are significant changes in both the intensity and location of the jet stream. In June, the core of EAJS is located over South Korea and southern Japan. It shifts poleward in July, and is finally located over Northeast China and the La Perouse Strait in August.

Climatologically, the EAJS experiences an obvious seasonal evolution in its meridional location and intensity (Fig. 2). The core of the EAJS is located approximately at 32.5°N in January, shifts northward slowly in winter and distinctly in spring, and reaches its highest meridional degree (about 45°N) in late July-early August. Afterwards, the core moves southward swiftly, and returns to 32.5°N at the end of year. During summer, the EAJS core experiences the most rapid change in meridional location, and this location change includes both poleward and equatorward shifts. Figure 2 also shows that the EAJS is strongest in winter (with maximum velocity over 70 m s^{-1}) and becomes weakest in summer (with maximum velocity below 30 m s^{-1}).

Figure 3 shows the patterns of eigenvectors of the first two leading modes from the EOF analysis of U200 over East Asia in JJA, June, July, and August. In each month and in JJA, the first mode (EOF-1) exhibits a meridional out-of-phase structure, with positive values in the south extent and negative values in the north extent. These positive and negative values are approximately of the same amounts, and the zero lines are located roughly at the same latitudes as the climatological EAJS cores in June, July, August, and JJA, respectively. On the other hand, in each month and in JJA, the second mode (EOF-2) exhibits a sandwich-like structure in the meridional direction, with positive

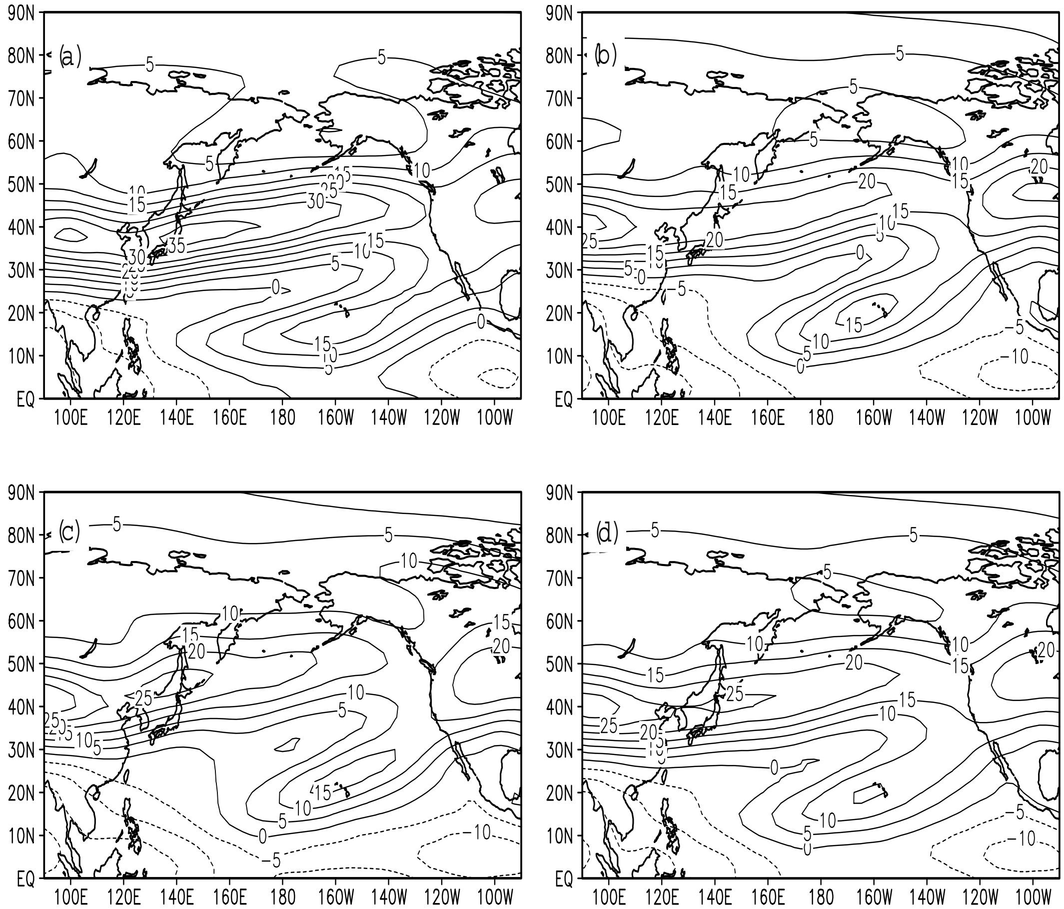

Fig. 1. 1979–2002 mean 200-hPa zonal wind (m s^{-1}) in (a) June, (b) July, (c) August, and (d) JJA.

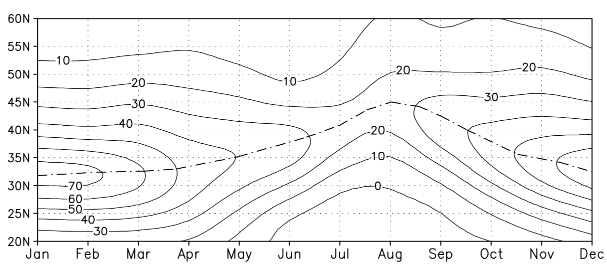

Fig. 2. The latitudinal distribution of climatological U200 (m s^{-1}) averaged between 120°E and 150°E. The dot-dashed line delineates the EAJS core.

Table 1. The explainable variance of the first two leading EOF modes' principal components of U200 in JJA, June, July, August and the correlation between the corresponding PC-1 and the EAJS Index (EAJSI).

	JJA	Jun	Jul	Aug
EOF-1	47.1%	47.2%	51.8%	48.7%
EOF-2	24.2%	20.5%	21.9%	27.5%
CORR(PC-1, EAJSI)	0.94	0.98	0.90	0.98

values in the middle and negative values to the south and north. The centers of the positive values are roughly at the same latitudes as the climatological EAJS cores in each month and in JJA, respectively.

According to the first two principal components of the EOF analysis for each month and in JJA, respectively, we performed a composite analysis. We chose the cases for when the absolute values of the principal components are greater than 0.5. The number of chosen cases ranges from 6 to 9. Figure 4 shows the composite U200 averaged between 120°E and 150°E. The left panels, which are for the first mode, clearly show that the EAJS tends to shift equatorward for the positive cases compared with the negative cases in each month and in JJA. This confirms that the first mode (EOF-1) features the meridional displacement of the EAJS. Particularly, in July, the EOF-1 delineates not only the meridional displacement but also the change of intensity. The right panels, which are for the second mode, show that the EAJS exhibits a strong intensity change and little meridional displacement in each mon-

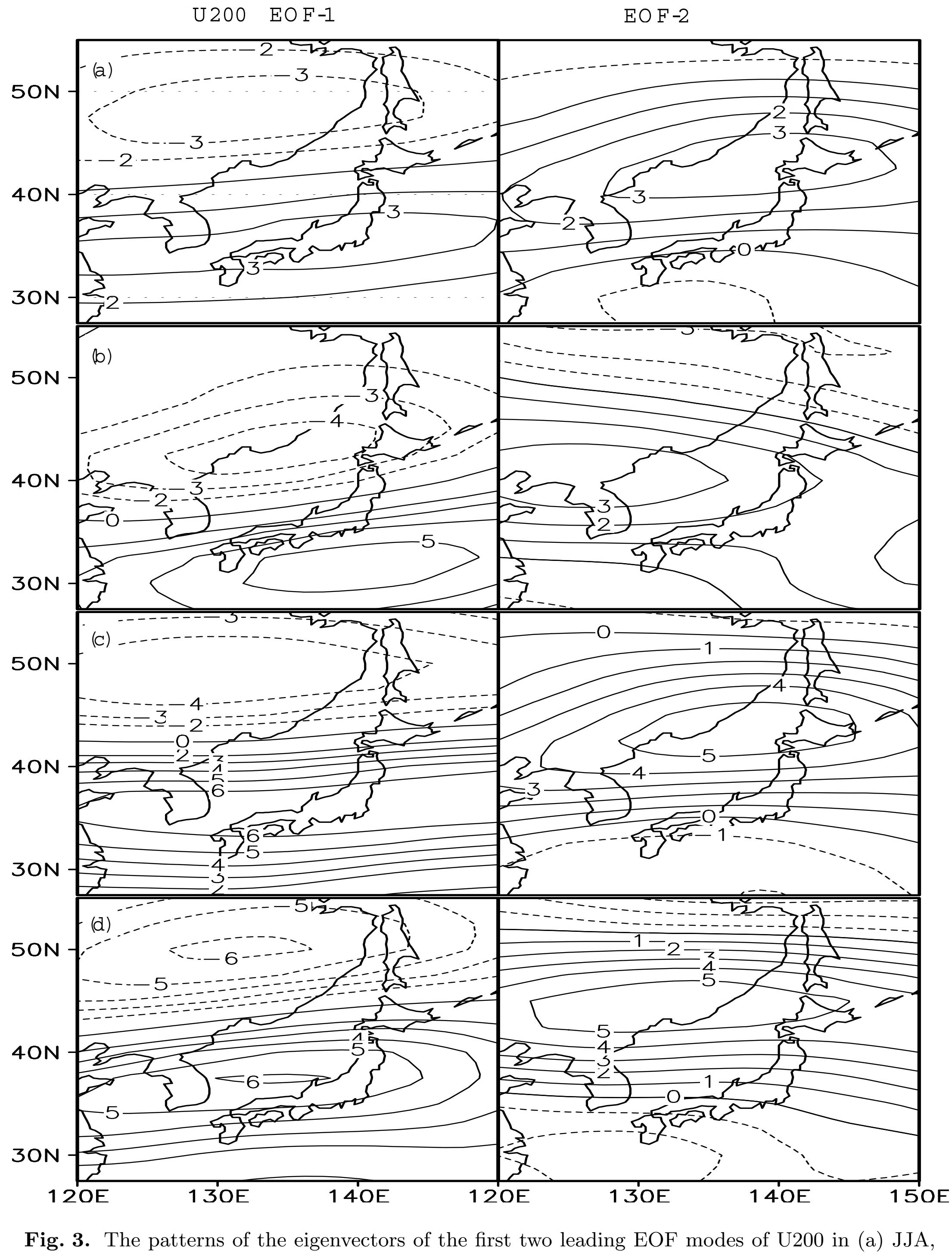

Fig. 3. The patterns of the eigenvectors of the first two leading EOF modes of U200 in (a) JJA, (b) June, (c) July, and (d) August.

th and in JJA. Thus, the second mode features the intensity of EAJS. Whether in JJA, June, July, or August, the first mode explains about half of the U200 total variance, and the second mode explains about 20%–25% (Table 1). The first two modes can totally account for about 70% of the U200 variance. This demonstrates that the variance of U200 over East Asia in summer mainly results from the displacement in the meridional direction and from the intensity change of EAJS, and the meridional displacement is the most remarkable feature of the interannual variability in EAJS.

3. Circulation anomalies associated with the meridional displacement of the EAJS

To describe the year-to-year meridional displacement of the EAJS, a JJA EAJS index is defined by the U200 difference averaged between the two regions: 10 degrees equatorward and poleward of the JJA-mean EAJS core within the longitude band of 120°–150°E, similar to that of Lu (2004). The JJA EAJS index actually depicts the mean meridional shear of U200 around the core of the climatological JJA EAJS. Yearly values of the EAJS index are shown in Fig. 5. The five years with the highest values are 1980, 1982, 1989, 1993, and 1998, and the five years with lowest values are 1981, 1984, 1985, 1990, and 1994. These ten years will be used for a composite analysis.

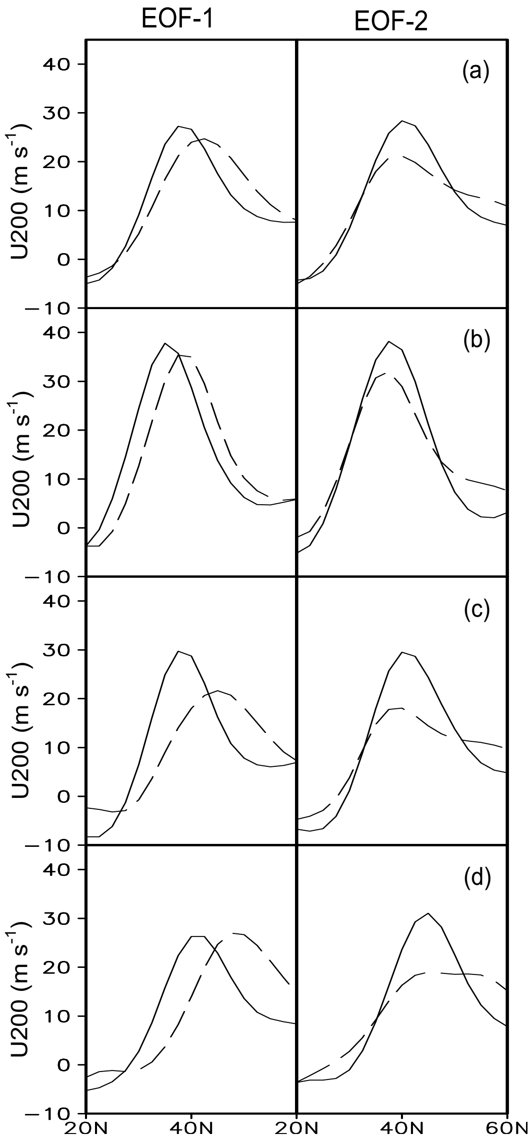

Fig. 4. Composite U200 averaged between 120°E and 150°E for the first (left) and the second (right) mode of the EOF analysis of (a) JJA, (b) June, (c) July, (d) August U200 over East Asia, respectively. The solid (dashed) lines show the average U200 over 120°–150°E in the years when the values are larger (smaller) than 0.5 (–0.5). Units: m s^{-1}.

Figure 6 shows the composite differences of zonal wind at 200 hPa between the five years with highest values and the five years with lowest values. Figure 6d shows that the JJA-mean U200 differences exhibit a significantly dissymmetric distribution along the belt about 40°N over East Asia, and the strongest westerly (easterly) anomaly appears to the south (north) of the JJA-mean EAJS core. It is revealed that a similar dissymmetric distribution exists in July (Fig. 6b) and August (Fig. 6c). In June, however, the strongest westerly (easterly) anomalies appear over the eastern Pacific and North America (not shown in Fig. 6a), and only very weak dipole-like anomalies appear over East Asia. Thus, this indicates that the anomalies of U200 in July and August, rather than in June, significantly contribute to the JJA EAJS index.

To confirm that the EAJS index can depict the meridional displacement of the EAJS, a composite analysis is performed in a similar way as that used to draw Fig. 4. Figure 7 shows the composite results. The cores of the EAJS for positive index years are clearly located to the south of those for negative index years in JJA, July, and August, but weakly in June. It is also worth noting that Fig. 7c and 7d show that the JJA EAJS index depicts not only the meridional displacement but also the intensity change of the EAJS in July and August, and when the EAJS moves southward, the intensity of U200 over East Asia is increased in July (Fig. 7c), but decreased in August (Fig. 7d). Therefore, it is necessary to separately analyze the meridional displacements of the EAJS month by month in summer.

In a way similar to the definition of the JJA EAJS index, we define three monthly EAJS indexes with the cores set to 37.5°N for June, 40°N for July, and 45°N for August, respectively. The time series of the three EAJS indexes, which are for (a) June, (b) July, and (c) August from 1979 to 2002 are shown in Fig. 8. Compared to the first principal component (PC-1) from the EOF analysis of U200, the monthly PC-1 is significantly correlated to the corresponding monthly EAJS index. That is, the June PC-1 is significantly associated with the June EAJS index, the July PC-1 is significantly associated with the July EAJS index, and

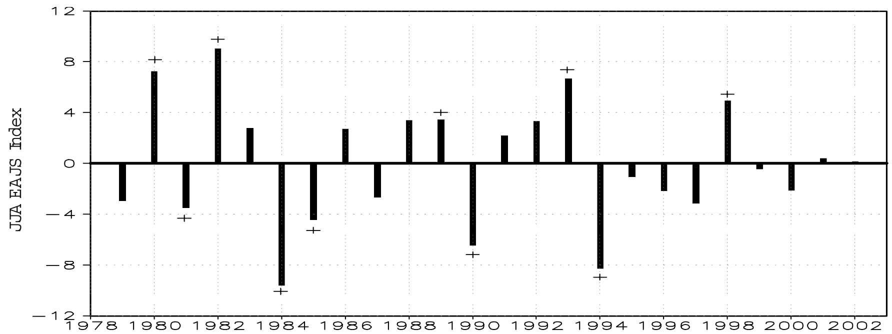

Fig. 5. Interannual variations of the JJA EAJS index from 1979 to 2002. This index is defined by the difference between the 200-hPa zonal winds (m s^{-1}) averaged over the two regions that cover the 10 degrees poleward and equatorward of the EAJS core within the longitudes of 120°–150°E (equatorward minus poleward), to describe the meridional displacement of the JJA-mean EAJS. The EAJS core is set to 40°N. The five years of the highest values and the five years of the lowest values, which are taken for a composite study, are indicated by cross marks.

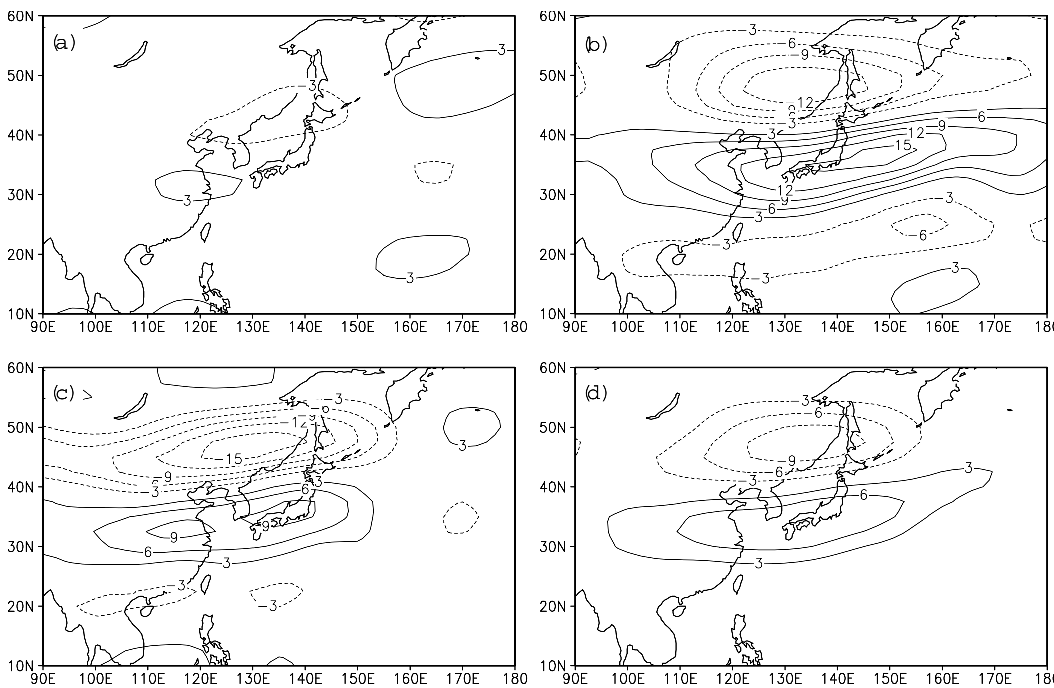

Fig. 6. Composite differences of U200 (m s^{-1}) between high and low JJA EAJS index years for (a) June, (b) July, (c) August, (d) JJA.

the August PC-1 is significantly associated with the August EAJS index from 1979 to 2002 with correlation coefficients of 0.98, 0.9, and 0.98, respectively (Table 1). The significant correlations reveal that the three monthly EAJS indexes are appropriate to delineate the meridional displacement of the EAJS. On the other hand, the composite U200 averaged between 120°E and 150°E for the June, July, and August EAJS indexes displays a similar distribution to that in Figs. 4b–4d, respectively (figure is not shown here). This similarity suggests the same conclusion as that indicated by the study of correlations between the PC-1s and the three monthly EAJS indexes, that is, the three monthly EAJS indexes accurately delineate the monthly meridional displacement of the EAJS in summer.

To reveal the anomalies of atmospheric circulation associated with the monthly meridional displacement of the EAJS in summer, we perform a composite analysis on the five cases of the highest indexes and five

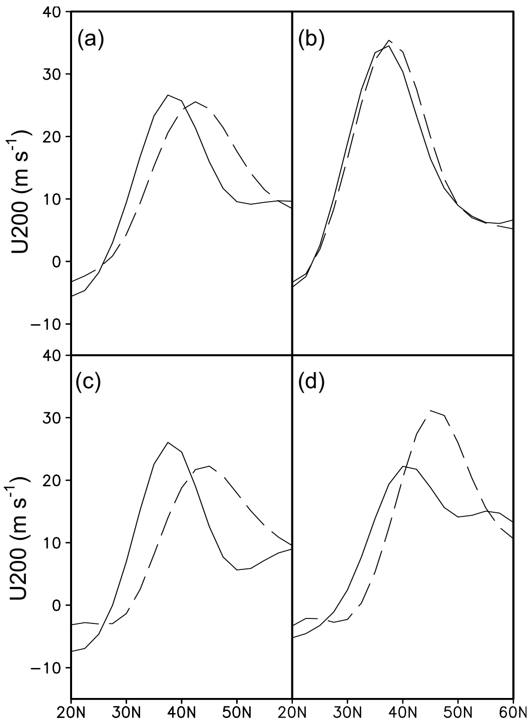

Fig. 7. Same as Fig. 6, but for U200 (m s^{-1}) averaged over 120°–150°E.

cases of the lowest indexes, respectively. The five years of the highest index are 1982, 1983, 1988, 1992, and 1995 for June; and 1980, 1982, 1983, 1989, and 1993 for July; and 1980, 1981, 1987, 1993, and 1998 for August, and the five years with the lowest index are 1979, 1984, 1990, 1991, and 1996 for June; 1981, 1984, 1985, 1994, and 2001 for July; and 1982, 1984, 1985, 1994, and 1999 for August.

Figure 9 shows the composite differences of U200 according to the monthly indexes for June, July and August, respectively. As one expects, the figure is covered with shading (indicating areas exceeding the 95% significance level determined by the two-sided Student's *t*-test), over East Asia and the western North Pacific in each month. The anomalous westerly (easterly), shaded over East Asia and the western Pacific is located to the south (north) of the core of the climatological EAJS, indicating that the EAJS migrates southward when the index is positive. Thus, these monthly EAJS indexes are appropriate to describe the monthly meridional displacement of the EAJS in summer. In June, the shadings also appear over the eastern North Pacific and North America, which suggests that the meridional displacement of EAJS in this month is associated with substantial remote circulation anomalies. In August, the shading also appears

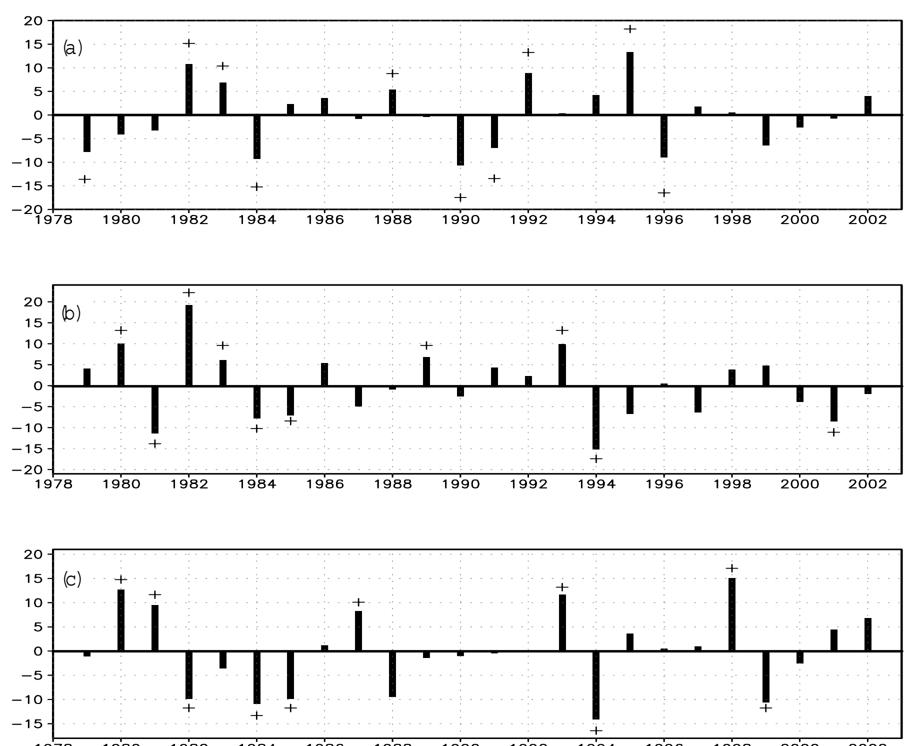

Fig. 8. Same as Fig. 5, but the EAJS core is set to 37.5°N, 40°N, and 45°N for (a) June, (b) July, and (c) August, respectively.

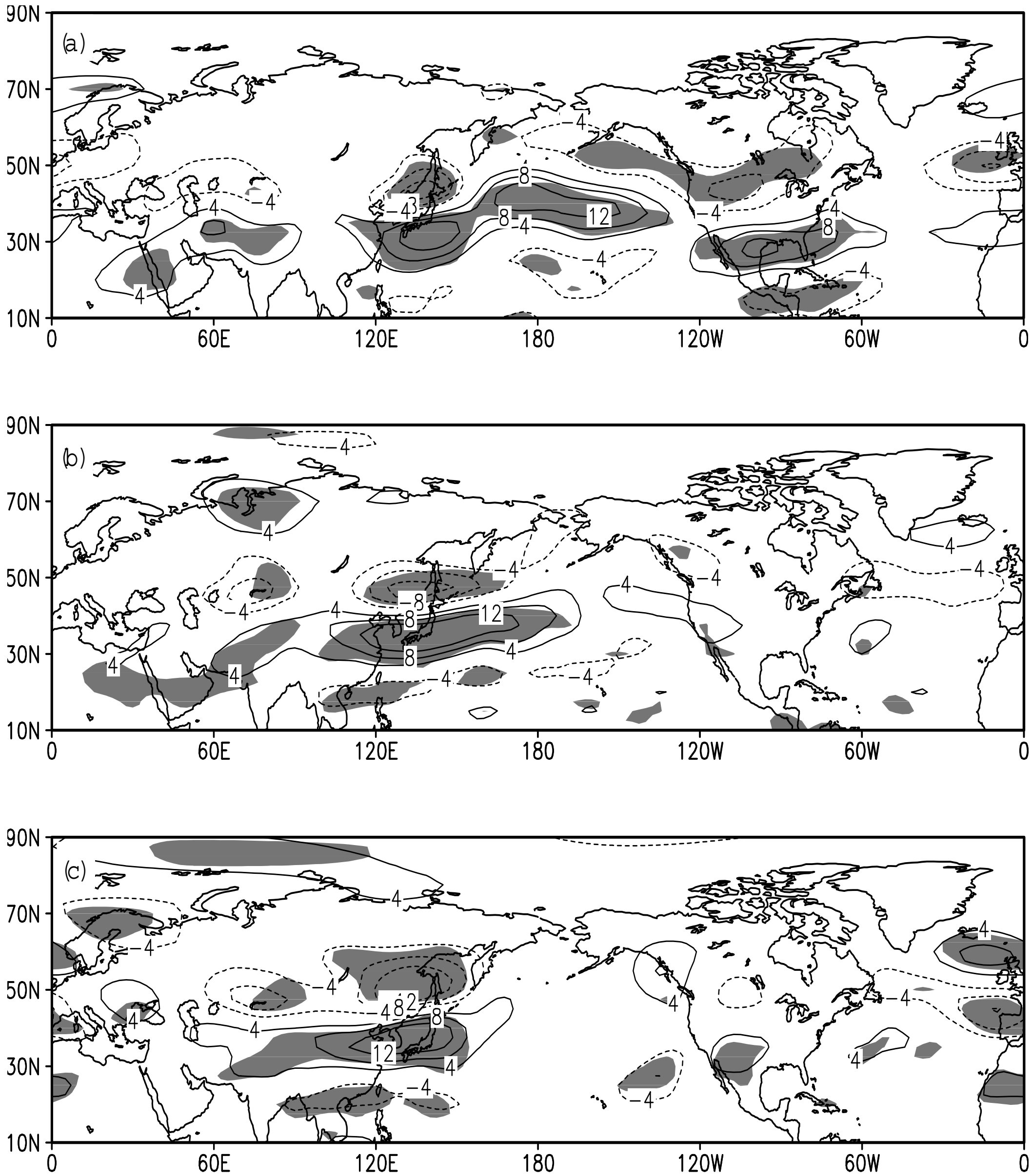

Fig. 9. Composite differences (positive minus negative EAJS indexes) of U200 at (a) June, (b) July, and (c) August according to the corresponding EAJS index. The shading illustrates the significance of the differences at the 95% level determined from the two-sided Student's t-test. Contour interval is 4 m s^{-1}.

over the North Atlantic and Western Europe.

Composite 100-hPa geopotential heights (H100) over Asia and the Northwest Pacific in June, July and August are shown in Fig. 10. The SAH at 100 hPa has a weak change, corresponding to the meridional displacement of EAJS, in June (Fig. 10a). In July and August, however, the SAH is shifted southeastward over East Asia and the Northwest Pacific when the EAJS is located equatorward (Figs. 10b and 10c). Compared with the remarkable monthly differences in the shape of the SAH related to the southward displacement of the EAJS, the anomaly pattern is similar among each monthly figure, with negative anomalies over East Asia and the Iran Plateau in all months of summer corresponding to a southward displacement of the EAJS (Fig. 11). It seems that the weak negative anomaly in East Asia in June (Fig. 11a) also contributes slightly to the weak and southward-located SAH. The negative anomaly center over East Asia seems to be displaced somewhat northward from

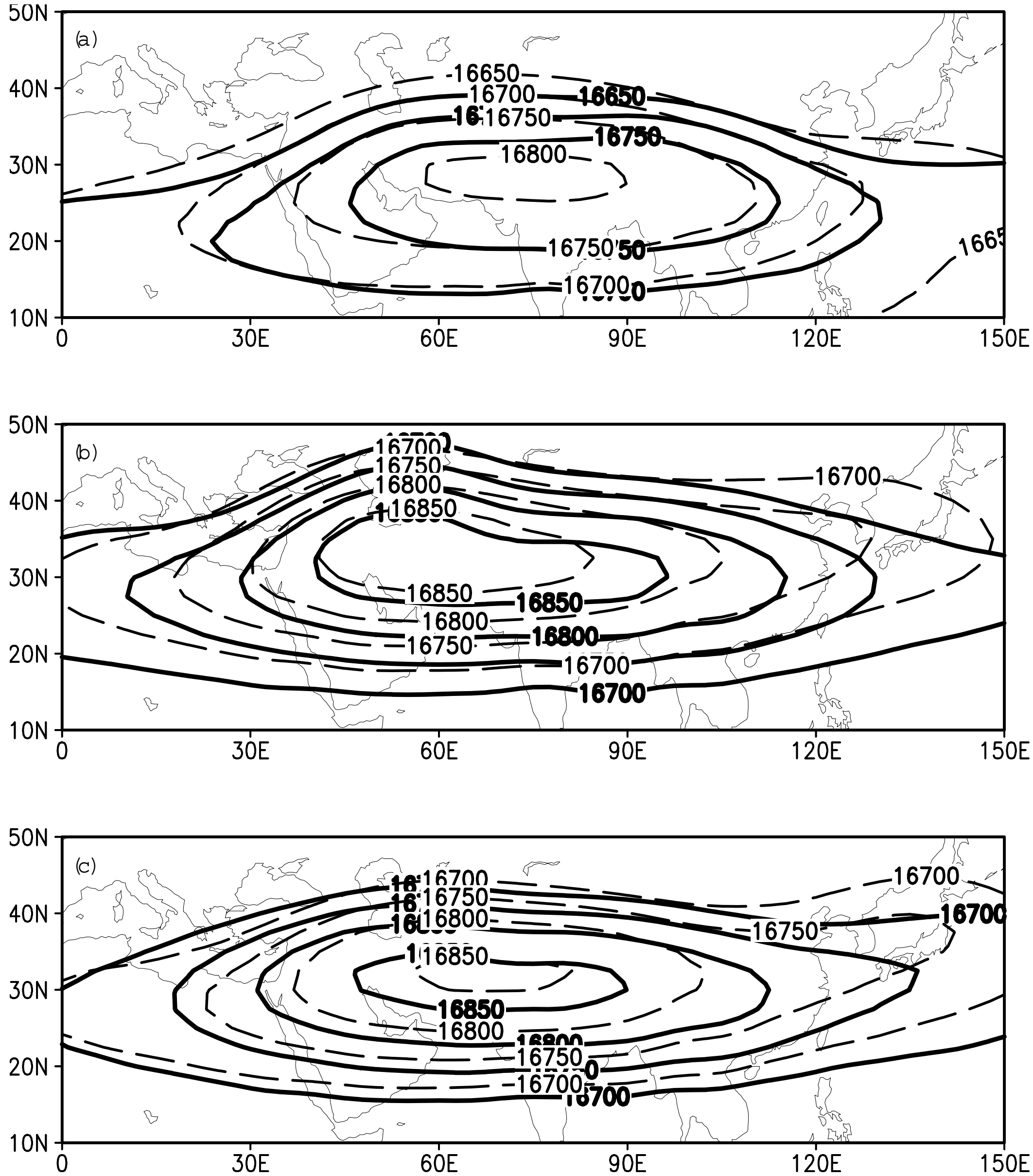

Fig. 10. Composite SAH at 100 hPa in (a) June, (b) July, (c) August. The solid (dashed) line delineates the 100-hPa geopotential heights in the high (low) EAJS years. Contour interval is 50 gpm.

June to August corresponding to the seasonal northward displacement of the EAJS. It also should be noted that over the Arabian Peninsula, in June (Fig. 11a) and July (Fig. 11b) only the negative anomaly appears corresponding to the meridional shift of the jet there shown in Figs. 9a and 9b.

WNPSH is a dominant feature in the lower troposphere and greatly influences the climate anomalies in East Asia. In this study, we use 850-hPa geopotential heights (H850) and horizontal winds to delineate the change of the WNPSH accompanying the monthly meridional displacement of the EAJS in summer.

Figure 12 shows the composite H850 in June, July and August, based on the monthly EAJS index, and the dark (light) shading illustrates the regions of positive (negative) anomalies of H850 at the significance level of 95%. Corresponding to the EAJS's equatorward displacement, significant negative anomalies of H850 appear over the subtropical Northwest Pacific in June and appear over Korea and Japan in August. In

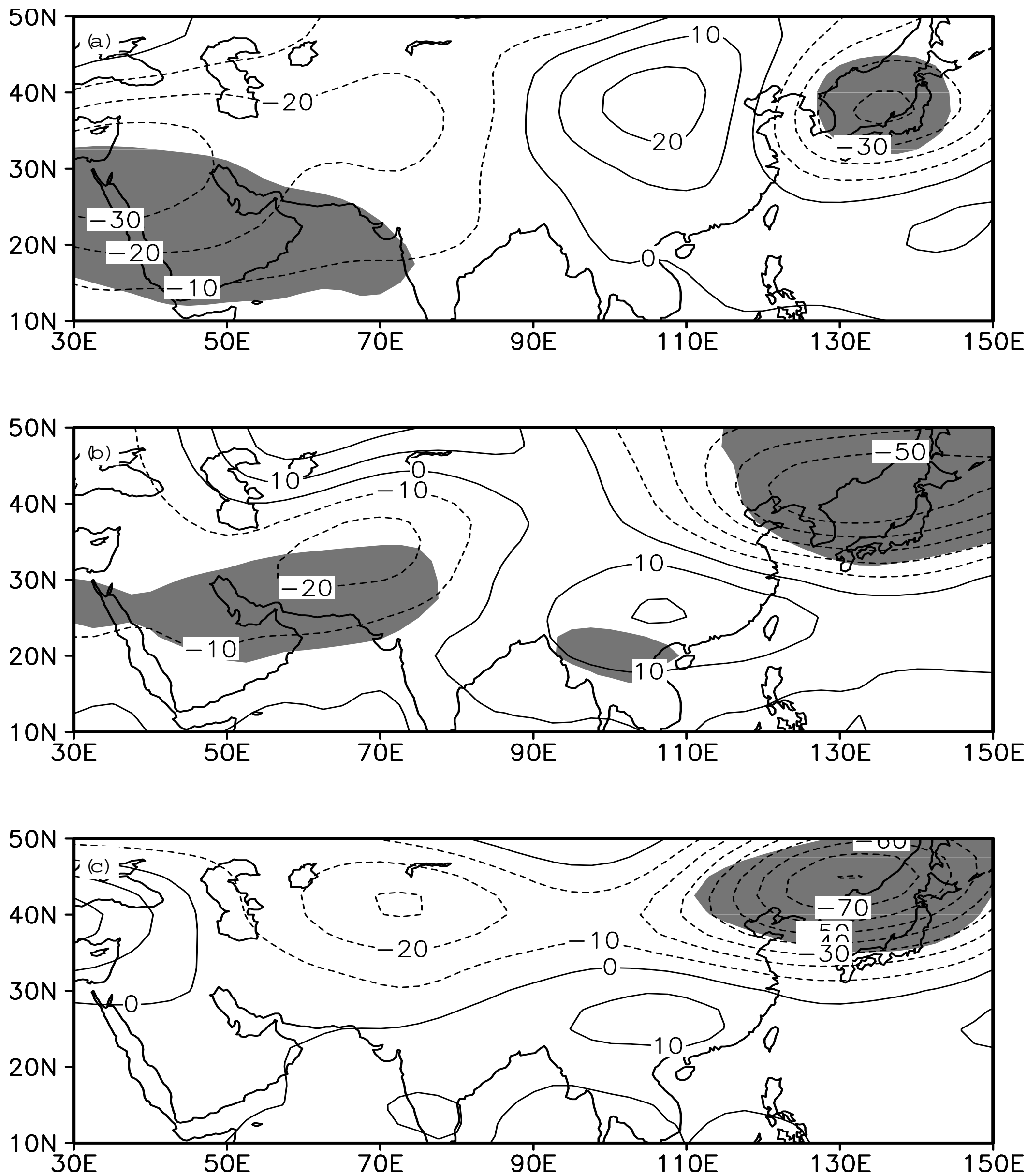

Fig. 11. Same as Fig. 9, but for 100-hPa eddy geopotential heights, which have had the zonal average removed. Units: gpm.

both months, these significant negative anomalies are exactly located at the north edge of the WNPSH, which shifts poleward significantly from June to August. Thus, the WNPSH exhibits an equatorward displacement, corresponding to the EAJS's equatorward displacement (indicated by the contour lines in Figs. 12a and 12c). Such an equatorward displacement of the WNPSH exists also in July, but not at the 95% significance level (Fig. 12b).

The composite differences of the 850-hPa winds (Fig. 13) show that there are cyclonic anomalies in the subtropical Northwest Pacific and East Asia. The locations of these cyclonic anomalies shift poleward from June to August, in agreement with the poleward shift of the WNPSH. The cyclonic anomaly in July is weaker, being consistent with the results shown by the 850-hPa height anomalies. On the other hand, it is is clear that the anomalous cyclone over South Japan in June and August, and the convergent belt over the Yangtze River and the Yellow River valleys in July and August, may bring heavy rainfall along the East Asian summer rainy belt, which correspond well with the areas of significantly positive correlation between the EAJS meridional displacement and the outgoing

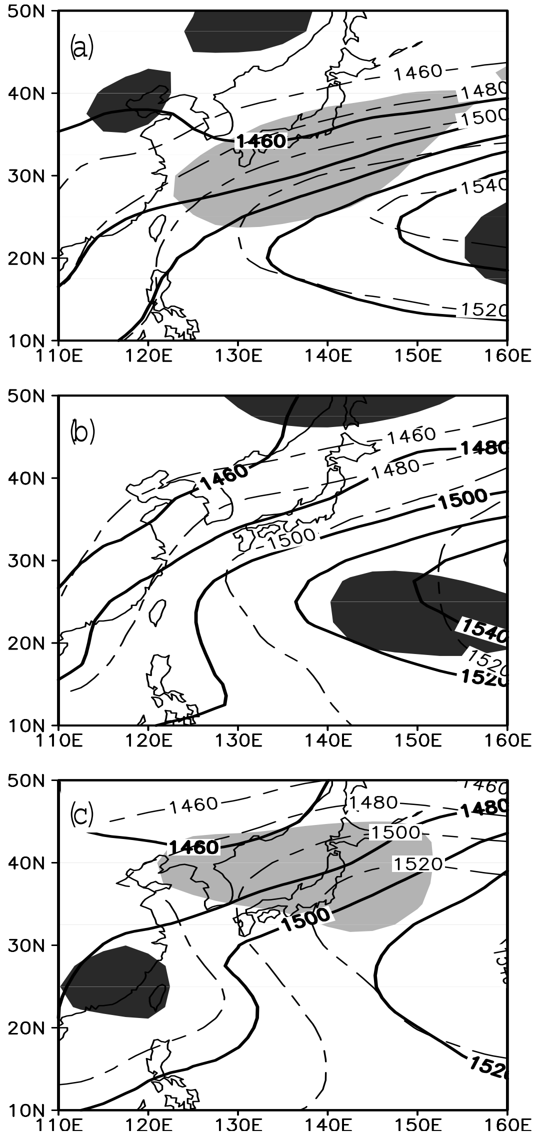

Fig. 12. Composite 850-hPa geopotential heights over East Asia and the Northwest Pacific for positive (solid line) and negative (dashed line) EAJS indexes of (a) June, (b) July, and (c) August. The dark (light) shading illustrates the significance of the positive (negative) 850-hPa geopotential height anomaly at the 95% significance level. Units: gpm.

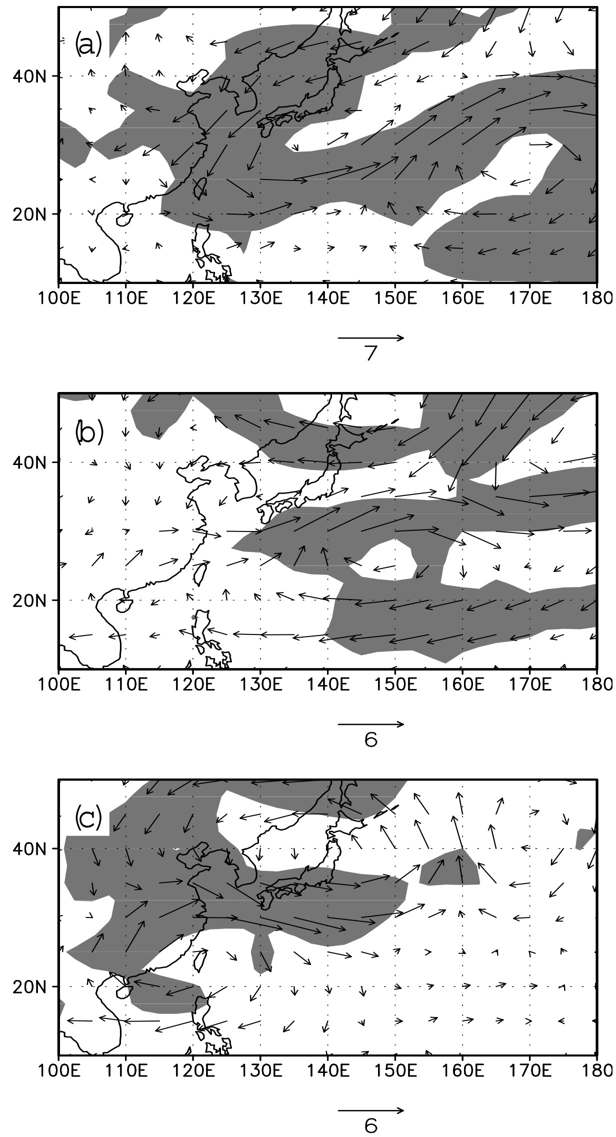

Fig. 13. Same as Fig. 9, but for 850-hPa winds. The area where either the zonal wind or meridional wind at 850 hPa is significant at the 95% level is shaded. Units: m s^{-1}.

longwave radiation (OLR) in June, July, and August (Lu, 2004).

4. Conclusion

Monthly data, which include geopotential height and winds from NCEP/DOE reanalysis-2, are employed to analyze the interannual meridional displacement of the EAJS in summer. The EOF analysis of U200 shows that the eigenvector patterns of the first two modes, which can explain most of the total variance, are able to delineate the displacement in the meridional direction and the changes of intensity. The meridional displacement of the EAJS is the most remarkable feature of U200 variability over East Asia and the Northwest Pacific in each month of summer and in summer as a whole.

The composite results show that the JJA-mean EAJS index, which is used to describe the anomalous meridional displacement of the JJA-mean EAJS, can only effectively depict the zonal wind anomalies over East Asia at 200 hPa in July and August but not in June. In order to investigate the influence on the atmospheric circulation anomalies associated with the meridional displacements of EAJS, it is necessary to define an EAJS index for each month in summer.

The composite differences of the geopotential heights at 100 hPa show that when the EAJS shifts equatorward, the SAH withdraws southeastward significantly in July and August, but weakly in June. The present study shows that there is a link between the northwestern and northeastern extents of the South Asian high. Latent heating over South Asia may induce Rossby-type circulation at the upper troposphere, and thus affect the northwestern extent of the South Asian high. On the other hand, the northeastern extent of the South Asian high, or the East Asian upper-tropospheric westerly jet stream, is closely associated with the tropical heating over the Philippine Sea through the strong meridional interaction (Lau et al., 2000; Lu, 2004). Therefore, the link between the northwestern and northeastern extents of the South Asian high may be caused by the tropical heatings. However, some studies have suggested that the connection between the East and South Asian monsoons is accomplished through the mid-latitude circulation wave pattern (Krishnan and Sugi, 2001; Lu et al., 2002; Wu, 2002). Thus, the mechanism responsible for the link between the northwestern and northeastern extents of the South Asian high, or for the relationship between the South Asian high and East Asian upper-tropospheric westerly jet stream, remains an interesting future research topic.

On the other hand, corresponding to the equatorward displacement of the EAJS, the WNPSH exhibits a significant equatorward displacement in June and August, but not in July. However, the reason for this monthly difference is still unknown and requires further research.

Acknowledgments. The authors would like to thank the two anonymous reviewers for their comments. This work was supported by the Chinese Academy of Sciences (Grant No. KZCX3-SW-221) and the National Natural Science Foundation of China under Grant No. 40221503.

REFERENCES

Bell, G. D., and Coauthors, 2000: Climate assessment for 1999. *Bull. Amer. Meteor. Soc.*, **81**, 1–50.

Ding Yihui, 1992: Summer monsoon rainfalls in China. *J. Meteor. Soc. Japan,* **70**, 373–396.

Dole, R. M., and R. X. Black, 1990: Life cycles of persistent anomalies. Part II: The development of persistent negative height anomalies over the North Pacific Ocean. *Mon. Wea. Rev.*, **118**, 824–846.

Dong Min, Yu Jianrui, and Gao Shouting, 1999: A study of the variations of the westerly jet over East Asia and its relation with the tropical convective heating. *Chinese J. Atmos. Sci.*, **23**, 62–70. (in Chinese)

Gao Shouting, and Tao Shiyan, 1991: Acceleration of upper-tropospheric jet stream and low-tropospheric frontogenesis. *Chinese J. Atmos. Sci.*, **15**, 11–21. (in Chinese)

Hou, A. Y., 1998: Hadley circulation as a modulator of the extratropical climate. *J. Atmos. Sci.,* **55**, 2437–2457.

Kanamitsu, M., W. Ebisuzaki, J. Woollen, S-K Yang, J.J. Hnilo, M. Fiorino, and G. L. Potter, 2002: NCEP-DOE AMIP-II Reanalysis (R-2). *Bull. Atmos. Meteor. Soc.*, **83**, 1631–1643.

Krishnan, R., and M. Sugi, 2001: Baiu rainfall variability and associated monsoon teleconnections. *J. Meteor. Soc. Japan*, **79**, 851–860.

Kung, E. C., and P. H. Chan, 1981: Energetic characteristics of the Asian winter monsoon in the source region. *Mon. Wea. Rev.*, **109**, 854–870.

Lau, K. M., and J. S. Boyle, 1987: Tropical and extratropical forcing of the large-scale circulation: A diagnostic study. *Mon. Wea. Rev.*, **115**, 400–428.

Lau, K.-M., K.-M. Kim, and S. Yang, 2000: Dynamic and boundary forcing characteristics of regional components of the Asian summer monsoon. *J. Climate*, **13**, 2461–2482.

Lu Riyu, Jai-Ho Oh, Beak-Jo Kim, Hee-Jeong Beak, and Huang Ronghui, 2001: Associations with the interannual variations of onset and withdrawal of the Changma. *Adv. Atmos. Sci.*, **18**, 1066–1080.

Lu, Riyu, Jai-Ho Oh, and Beak-Jo Kim, 2002: A teleconnection pattern in the upper-level meridional wind over the North African and Eurasian continent in summer. *Tellus*, **54A**, 44–55.

Lu, Riyu, 2004: Associations among the components of the East Asian summer monsoon systems in the meridional direction. *J. Meteor. Soc. Japan*, **82**, 155–165.

Neyama, Y., 1963: On the dates of the transition of wind direction from west to east in the lower stratosphere at Marcus Island (24°17′N, 153°88′E) in late spring and the setting in of "Baiu" (the rainy season in Japan). *Geophys. Mag.*, **31**, 633–651.

Palmen, E., and C. W. Newton, 1969: *Atmospheric Circulation Systems: Their Structure and Physical Interpretation.* Academic Press, 603pp.

Tao Shiyan, and Chen Longxun, 1987: A review of recent research of the East Asian summer monsoon in China. *Monsoon Meteorology*, C.-P. Chang and T. N. Krishnamurti, Eds., Oxford University Press, 60–92.

Wu Guoxiong, Liu Xin, Zhang Qiong, Mao Jiangyu, Liu Yimin, Li Weiping, and Qian Yongfu, 2002: Progress in the study of the climate impacts of the elevated heating over the Tibetan Plateau. *Climatic and Environmental Research*, **7**, 184–201. (in Chinese)

Wu Renguang, 2002: A mid-latitude Asian circulation anomaly pattern in boreal summer and its connection with the Indian and East Asian summer monsoons. *J. Climate,* **22**, 1879–1895.

Yang, S., and P. J. Webster, 1990: The effect of summer tropical heating on the location and intensity of the extratropical westerly jet stream. *J. Geophys. Res.*, **95**, 18 705–18 721.

Yang, S., K.-M. Lau, and K.-M. Kim, 2002: Variations of the East Asian Jet Stream and Asian-Pacific-American winter climate anomalies. *J. Climate*, **15**, 306–325.

Yeh, T.-C., S.-Y. Tao, and M.-T. Li, 1959: The abrupt change of circulation over the Northern Hemisphere during June and October. *The Atmosphere and the Sea in Motion*, B. Bolin, Ed., Rockefeller Institute Press, 249–267.

Zeng Qingcun, 1979: *Mathematical and Physical Basis for Numerical Weather Forecast*. Science Press, 314pp.

Zhang Qiong, Wu Guoxiong, and Qian Yongfu, 2002: The bimodality of the 100 hPa South Asia High and its relation to the climate anomaly over East Asia in summer. *J. Meteor. Soc. Japan,* **80**, 733–744.

Zhang Yongshen, and Wu Guoxiong, 1999: Diagnostic investigation on the mechanism of the onset of Asian summer monsoon and abrupt seasonal transitions over the Northern Hemisphere. Part II: The role of surface sensible heating over Tibetan Plateau and surrounding regions. *Acta Meteorologica Sinica*, **57**, 56–73. (in Chinese)